

Comparison of the Computed Flow Field Around a Bubble Growing at an Orifice Using PIV Techniques

M.T. Stickland, W.M.Dempster

Department of Mechanical Engineering, University of Strathclyde, Glasgow,UK

Contact: Email:wdempster@mecheng.strath.ac.uk

ABSTRACT

For bubbles growing rapidly at orifices, the inertia of the liquid displacement and the resultant liquid flow field contribute to the production of an inertia force which tends to retard bubble movement. It is therefore the purpose of this paper to report on a study to examine the validity of liquid velocity fields predicted by potential flow methods and measurements made using Particle Image Velocimetry (PIV) techniques. Air bubbles are generated in water at atmospheric conditions from a 1 mm diameter orifice. The process is transient and occurs over a period of approximately 80 msec. Therefore a combination of high speed video techniques and PIV image processing has been used to determine the liquid velocity vector fields during the bubble growth, detachment and translation periods. This paper will present a summary of the experimental techniques and the theoretical model and discuss the results of the study.

1 INTRODUCTION

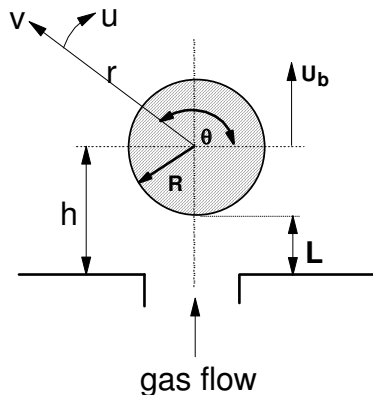
The transfer of mass and heat through direct interfacial processes is a common feature found in the process and nuclear industries and is either part of the normal operation of the plant or as a consequence of accident conditions. In general the sizing of mass and heat transfer equipment is determined by the overall heat transfer rates between mediums. However, these transfer rates are controlled at a micro level by the interfacial process between bubbles and liquid. In this study the attention is focused on the bubble generation mechanism which occurs at orifice plates. The mass and heat transfer processes largely depend on the initial bubble size as it flows into the bulk liquid. To be able to predict the heat and mass transfer

rates the bubble evolution has to be predicted and various different models are available, [1]. The basis of many theoretical models is in the assumption that the bubble is spherical and by application of a force balance acting on the bubble due to the main effects of buoyancy, surface tension, gas momentum effects and liquid inertia effects the motion of the bubble can be predicted. The assumption of a spherical bubble and the use of low viscosity fluids allows the application of irrotational flow approximations to calculate the liquid velocity field around the bubble as it expands from the orifice and is necessary to accurately calculate the retarding force acting on the bubble due to the liquid inertia. This force is believed to be one of the main forces that control the initial movement of the bubble and the condition when the bubble will detach from the orifice. However, the experimental data available to validate the mathematical models consists mainly of integrated parameters such as the time history of the bubble volume or to a more limited extent the volume at the point of detachment. These parameters though useful for overall validation do not indicate the appropriateness of the many details of the models, in particular the ability to properly calculate the liquid inertia force. The liquid force essentially can be related to the pressure distribution around the bubble as it changes during the bubble evolution. The pressure distribution can be determined via Bernoulli's equation and by calculating the liquid velocity around the bubble as it grows. Though the general problem relates to heat and mass transfer processes the basis of the hydrodynamic models required for modelling the general problem can be represented by air water systems. It is therefore the purpose of this paper to discuss a study which investigated the feasibility of using PIV techniques to determine the flow field around an air bubble as it grows and detaches from an orifice. The velocity field can then be compared to the theoretically calculated flow field to investigate the validity of the irrotational flow assumptions. In the proceeding sections the basis of the mathematical model is explained, the

experimental rig and PIV techniques are discussed, comparisons of theoretical and PIV images are presented and the issues that have arisen from the study will be discussed.

2. MATHEMATICAL MODEL

In this study the bubble is assumed to be spherical which allows the bubble movement and resulting liquid motion to be more mathematically amenable to an analytical approach. In this paper the intention is to determine the liquid velocity surrounding the bubble as the bubble grows into the liquid pool. The continuity equation is used to determine the bubble growth rate and the application of a force balance on the bubble allows the bubble acceleration to be determined. With these equations and application of kinematics allows the bubble position to be determined during the bubble generation period and combined with a analytical solution for the velocity potential function allows the velocity field to be determined. The solution procedure is outlined below.



If the bubble volume is taken as a control volume, as shown on Fig. 1, the application of the conservation of mass leads to the following equation, assuming constant density conditions

$$\frac{d(R)}{dt} = \frac{\dot{m}_a}{4\pi R^2 \rho_a} \quad (1)$$

Fig 1 bubble Control Volume R is the bubble radius , \dot{m}_a is the air mass flow at the orifice and ρ_a is the density of the incoming air.

The motion of the bubble is determined by a force balance where the contributing forces are assumed to be due to the excess pressure force, buoyancy, surface tension at the orifice, the reaction force by the surrounding liquid and the momentum of the incoming orifice air flow. In treating the motion of the bubble, the bubble is modelled generally as a linearly accelerating

control volume. The general form of the momentum equation relative to a stationary reference frame is discussed by Fox and MacDonald [2] and for the bubble motion can be reduced to

$$-F_L - F_\sigma + F_B + F_e = -M_a u_a + Ma \quad (2)$$

The forces on the left hand side of equation 2 are respectively the liquid reaction force, \mathbf{F}_L the surface tension force, \mathbf{F}_σ the bubble buoyancy, \mathbf{F}_B and the excess pressure force \mathbf{F}_e . The right hand side components are constructed from the rate of change of momentum in the control volume, the net change across the control volume and the acceleration of the control volume, respectively, u_a is the velocity of the air at the orifice flowing into the bubble. The evaluation of the forces $\mathbf{F}_e, \mathbf{F}_L, \mathbf{F}_\sigma$ and \mathbf{F}_B have to be considered carefully for accurate determination of the growth and detachment processes. \mathbf{F}_σ , the surface tension force at the orifice and \mathbf{F}_B is the buoyancy force are given by

$$F_e = \frac{\pi \sigma d_o}{2R} \quad F_\sigma = \pi d_o \sigma \sin \alpha \quad F_B = \frac{4\pi}{3} R^3 g (\rho_l - \rho_s) \quad (3)$$

In the test case studied in this paper the bubble contact angle α was measured from digital video images and was found to be approximately 60° and constant during the bubble growth. The most difficult force to calculate accurately is the liquid inertia force acting on the bubble. This force results from the combined effects of the pressure distribution and the shear stress due to the liquid motion around the bubble. For this study it has been assumed that the shear stress is negligible and therefore the total vertical force on the bubble due to the pressure distribution is calculated from

$$F_L = 2\pi R^2 \int_0^\pi P \sin \theta \cos \theta d\theta \quad (4)$$

By assuming an inviscid liquid velocity field the dynamic pressure distribution can be determined by applying Bernoulli's equation for an unsteady flow,ie

$$\frac{p}{\rho_l} = \frac{1}{2}|\bar{u}|^2 - \frac{\partial\phi}{\partial t} \quad (5)$$

The absolute velocity $|\bar{u}|^2$ of the liquid and the corresponding vector components are defined below in terms of the potential function ϕ

$$|\bar{u}| = \sqrt{u^2 + v^2} \quad u = \frac{\partial\phi}{\partial r} \quad v = \frac{1}{r} \frac{\partial\phi}{\partial\theta} \quad (6)$$

The velocity field around the bubble is determined by classical methods and are discussed by Milne [3], Ramsey [4], and Lamb [5], The theoretical approach that is applied here follows that of Wraith and Kakutani [6] who studied gas bubble formation. The bubble development is taken as a combination of two independent motions; an expansion process and a translation process. The expansion occurs throughout the process. However, during the period when the main bubble mass is attached to the orifice via a neck, the bubble is modelled as having an additional translation contributing to its motion. Since the fluid is assumed to be incompressible and irrotational the fluid velocity field can be described by a potential function ϕ which satisfies the Laplace Equation, $\nabla^2\phi = 0$. The analysis is rather lengthy and is explained in more detail by Arebi [7] however it will eventually lead to a potential function representing the fluid motion surrounding an expanding and translating sphere, as shown below.

$$\phi = R^2 \dot{R} \left[\frac{1}{r} + \frac{1}{2h} - \frac{r \cos\theta}{4h^2} + \frac{r^2}{16h^3} (3 \cos^2\theta - 1) \dots \right] + \frac{R^3}{2} \left[U_b - \frac{R^2}{4h^2} \left(\dot{R} - \frac{R}{2h} U_b \right) \right] \left[\frac{\cos\theta}{r^2} - \frac{1}{4h^2} + \frac{r}{4h^3} \cos\theta - \frac{3r^2}{32h^4} (3 \cos^2\theta - 1) \dots \right] + \quad (7)$$

$$\frac{R^7}{24h^3} \left[\dot{R} - \frac{3R}{4h} U_b \right] \left[\frac{1}{r^3} (3 \cos^2\theta - 1) \dots \right]$$

\mathbf{F}_L can now be found by substituting (7) into (6) and (5) to determine the pressure p. The relationship derived for p can then be substituted into equation (4) to determine an equation for

the liquid inertia force. When modelling the bubble growth using the assumption of a spherical geometry, it is necessary to account for the bubble necking process. In the model applied here a two stage process is implemented whereby the initial bubble motion is interpreted simply as a spherical bubble growing at a wall. Under these condition the bubble centre obeys the following kinematic relationships

$$h = R \quad U_b = \frac{dR}{dt} \quad a = \frac{d^2R}{dt^2}$$

when necking begins the bubble centre is interpreted as a combination of translation and expansion and the kinematic relationships are

$$h = L + R \quad U_b = \frac{dL}{dt} \quad a = \frac{dU_b}{dt}$$

The kinematic relationships can be integrated numerically to determine the bubble motion. The mathematical model discussed does not contain information to predict the detachment condition. However, since the objective of the study is to compare predicted and experimentally derived velocity fields the theoretical calculation is simply stopped at the experimentally determined detachment time.

3. EXPERIMENTAL TECHNIQUE

Particle image velocimetry is, now, a common technique which allows the whole flow field's velocity to be mapped instantaneously by computationally analysing a picture of the flow field. This image usually has multiple exposures of the flow which has been seeded with small particles and illuminated by a thin sheet of laser light. The analysis of a single image of the flow field is referred to as autocorrelation. An alternative to autocorrelation is to analyse two sequential images of the flow field; referred to as cross correlation. Cross correlation produces a vector map of the flow field by analysing pairs of sequential images. In this process the computer algorithm calculates the direction and magnitude of the displacement of

a particle, or group of particles, between exposures. If the time between exposures is known then, combined with an analysis of the direction of the displacement, the velocity of the particle and hence the flow in that region is known. This is shown on figure 2. Cross correlation analysis is advantageous because it does not create any directional ambiguity within the vectors calculated and is capable of measuring extremely low as well as a wide range of velocities. For information on PIV in general the reader is recommended to consult the paper by Gray [8].

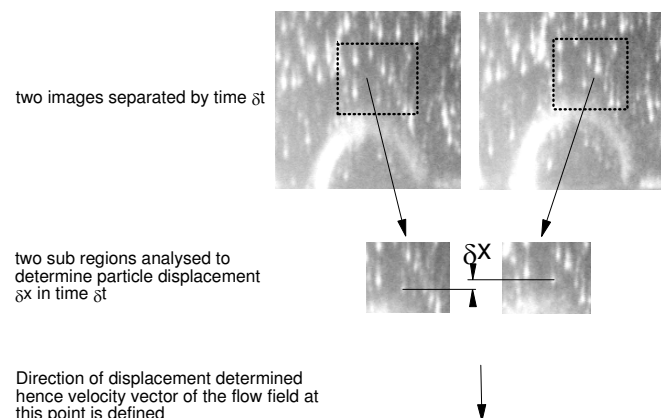


Figure 2: Cross correlation technique

The particles in the flow were illuminated by a laser sheet produced by a 5W Spectra Physics 165 Argon Ion laser and cylindrical lens. Typically only 2.5W of laser power were required for imaging purposes. The process of bubble formation was filmed by a Kodak Motioncorder high speed digital video camera which had a capability of recording at frame rates up to 600 frames per second. Air flow was provided by the lab high pressure air supply regulated to a lower pressure by a series of valves. The air was controlled by a needle valve situated upstream of the orifice. The water column was 150mm square section and 300mm high manufactured in glass with a 1 mm orifice at the base. A diagram of the experimental setup is shown in figure 3.

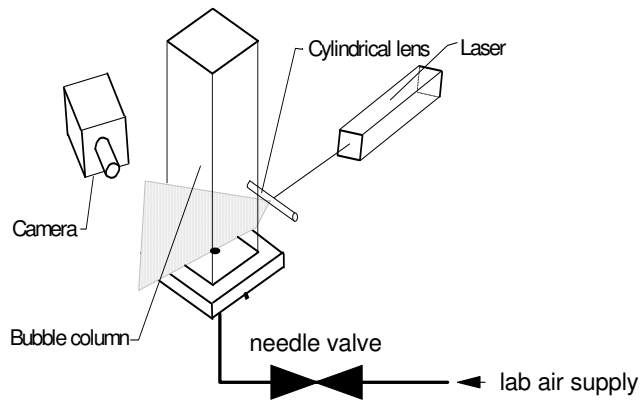


Figure 3 Experimental setup

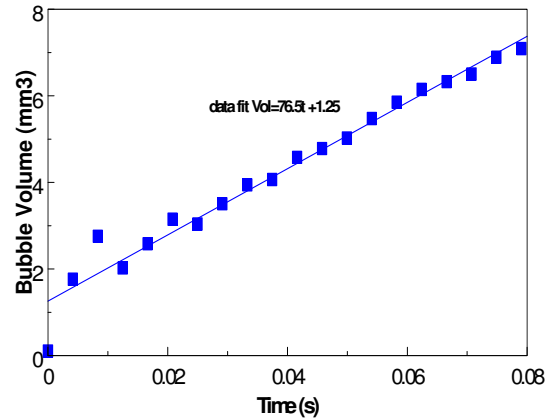


Figure 4 Bubble volume time history

Images were digitised by a Matrox frame grabber card in a 486DX266PC. The digitised images were analysed by Optical Flow Systems VidPiv PIV analysis Software by cross correlation on a Pentium P200 PC. To compensate for magnification within the optics a reference grid was filmed and digitised to give the required scaling information. When the acquired images had been digitised, pairs of images were analysed by cross correlation to yield the vector field around the emerging bubble. The images discussed in this paper were acquired at 240 frames per second. Timing is given from the first sign of bubble growth and the image is the first of the pair used for cross correlation.

Furthermore, from the digital video images of the bubble during the growth process, the time evolution of the bubble volume, surface area and centroid position were determined by analysing the images in each frame. From the analysed images the volume flowrate was determined for the test conditions as shown in Figure 4. It can be seen that the volume flowrate is constant over the bubble growth period and was calculated to be $76.5 \text{ mm}^3/\text{s}$.

4. RESULTS

The mathematical model was used to predict the experimental test discussed above. A comparison between the theoretical results and the experimental data are shown on Figs 5,6 and 7. Fig. 5 shows the experimentally measured bubble radius and the theoretically calculated value in conjunction with the bubble images recorded during the test. It can be seen that a reasonable prediction is achieved.

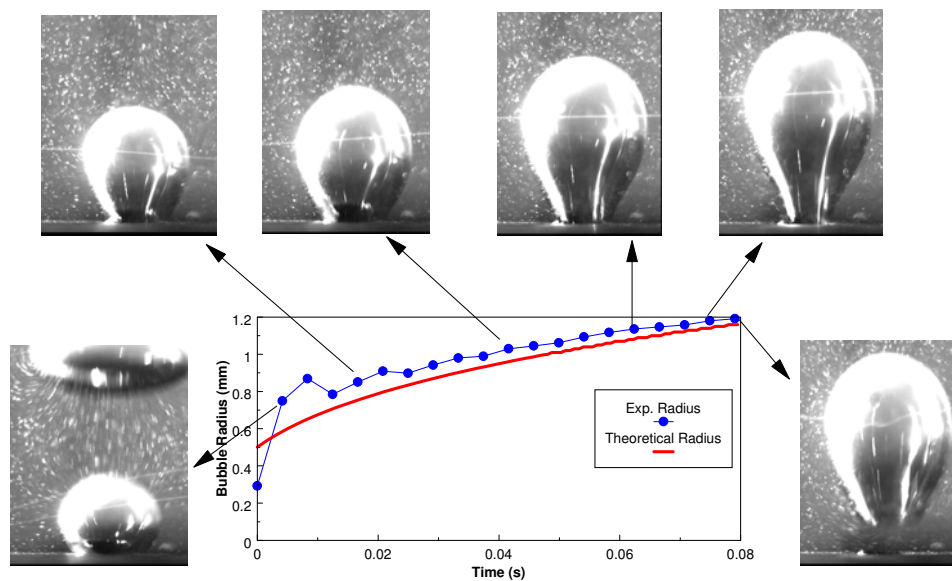


Figure 5 Comparison of experimental and predicted bubble radius

Figure 6 and 7 compare theoretical and experimentally derived bubble centroid position and surface area. The centroid position, which represents the movement of the bubble is not very well predicted by the theoretical model as can be seen in Fig 6. However, surprisingly the overall bubble surface area is well represented by a sphere as shown in Fig. 7

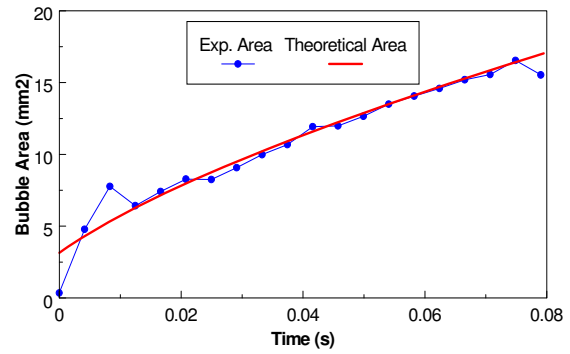
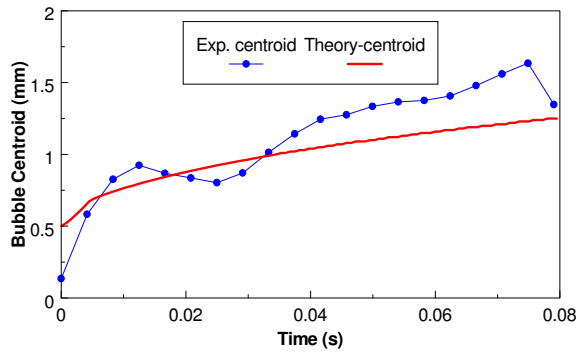


Fig. 6 Theoretical and exp. centroid position Fig. 7 Theoretical and exp. bubble area

While the reasonable predictions of bubble radius and surface area are reassuring, the relatively poor prediction of the centroid position is of significance due to the fact that the centroid position is indicative of the extent of bubble necking process and the effect of the resultant forces acting on the bubble. To further clarify these deficiencies a number of the predicted velocity fields have been compared with the PIV generated flow fields at 25, 50 and 75 msec during the bubble growth process and are shown on Figs 8a,8b and 8c The bubble detachment from the orifice occurs at approximately 77 msec.

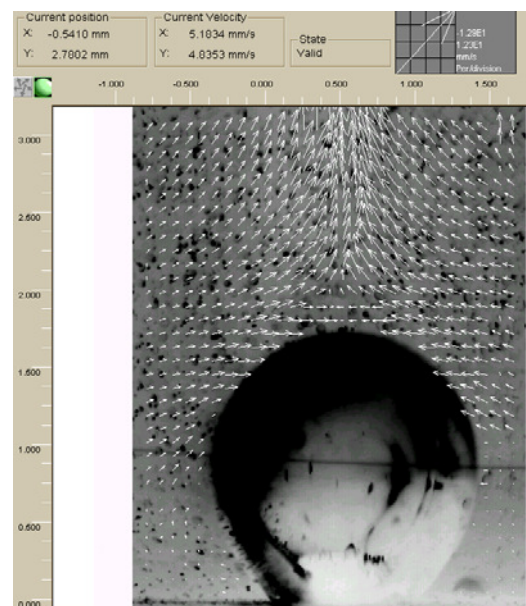
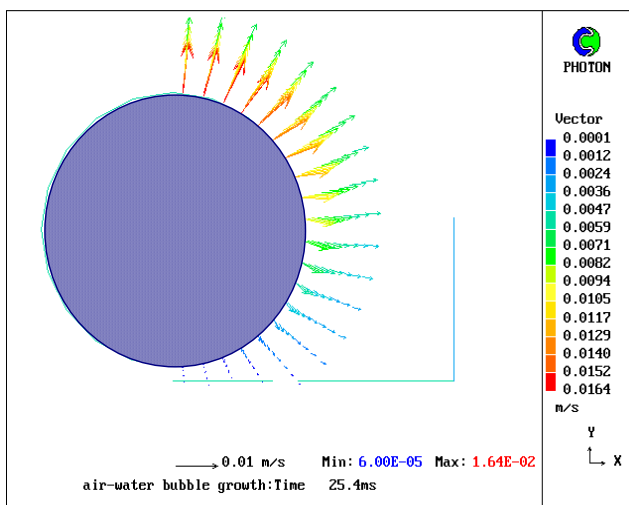


Fig 8a Experimental and predicted vector field at 25 msecs

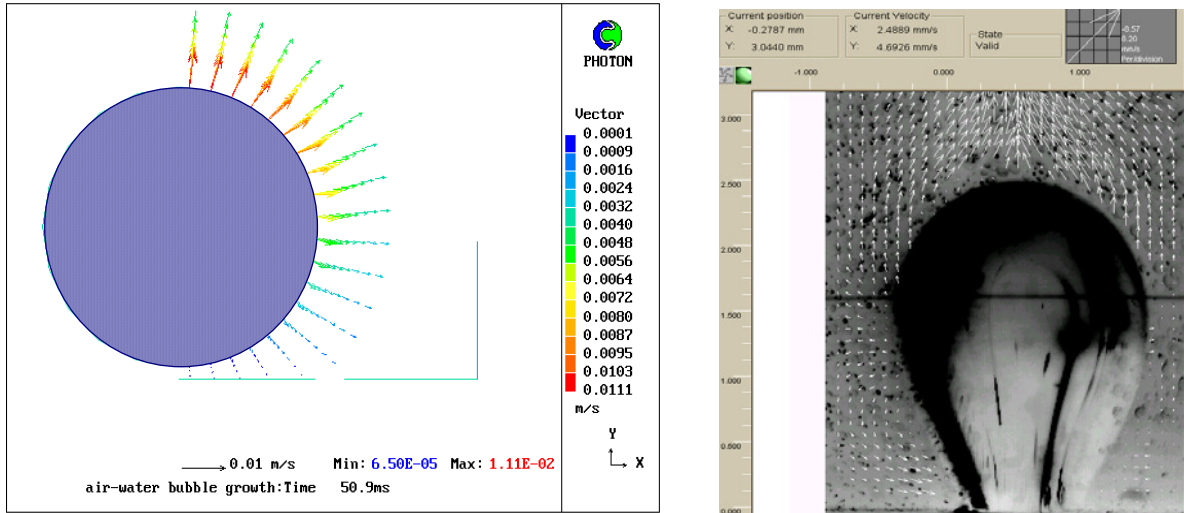
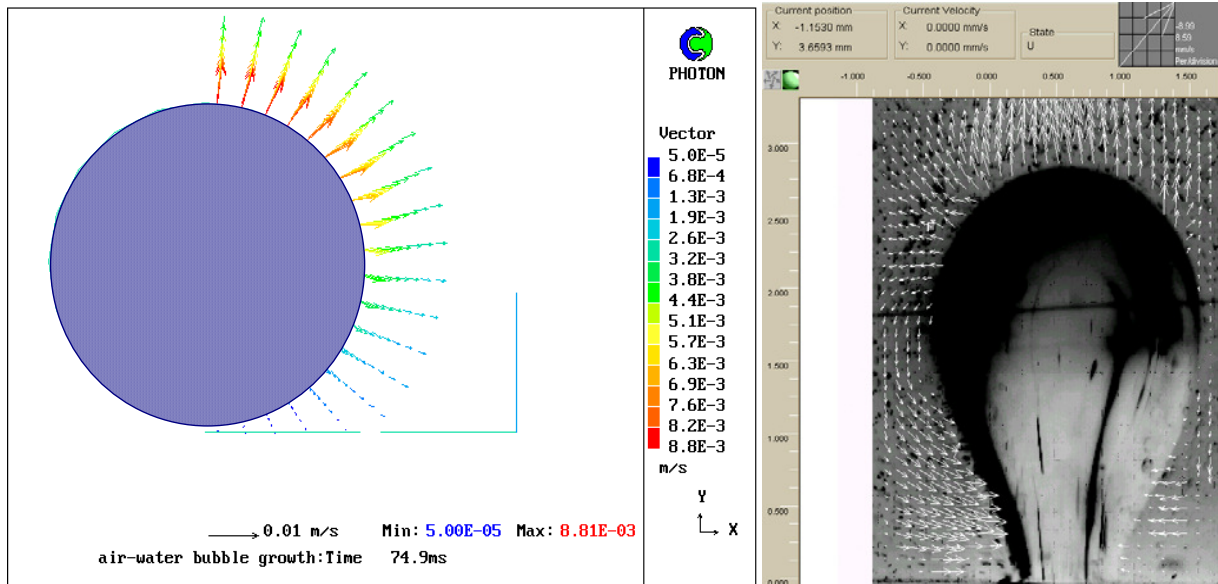


Fig 8b Experimental and predicted vector field at 50 msecs¹



¹ Note to reviewer. The above figures do not represent the details of the theoretical and experimental velocity fields as clearly as the authors would like and we intend to improve the images for a final version of the paper, if the paper is to the satisfaction of the reviewers.

Fig 8c Experimental and predicted vector field at 75 msec

The PIV images of the predicted velocity field coupled with the photographic images allow various features of the fluid flow to be ascertained. The velocity scaling for the predictions is given on the right hand side of the image while the scaling for the PIV plot is given in the top right hand corner. At present these images only allow a qualitative comparison when compared with the mathematical model. However, certain important features of the flow process surrounding the bubble can be discerned. In each of the figures the velocity field is predicted to be dominated by radial flows that decay quickly as the radius increases. In the PIV images much of the flow is dominated by a surrounding flow that has been generated by the displacements of the previously detached bubbles. The extent of the influence of these flows will depend on their magnitude compared with bubble surface values. For the test case presented here where the growth rate is very small the effect of this influence will be significant. It is also noticeable that the PIV images indicate a circulatory flow at the lower part of the bubble as it begins to neck. This is not predicted by the theoretical model to the same extent and is likely to be indicative of poor predictions of the liquid inertia effects. To better represent the circulatory nature of the flow with the current spherical model the translation of the bubble centroid has to be better predicted since this movement will induce an up flow beneath the bubble. Unfortunately, this movement will not be predicted without the correct calculation of the inertia force. It would therefore appear that for the case studied the applied modelling technique is not applicable.

5 CONCLUSIONS

A PIV technique has been developed to determine the velocity field around a bubble growing in water. The PIV images have been compared with predicted velocity fields based on a

mathematical model established from potential flow theory and indicate potential problems in the application in this type of modelling approach for air/water bubble growth problems.

6 NOMENCLATURE

a	bubble acceleration
A_b	bubble surface area
d_o	orifice diameter
F_B	buoyancy force acting on bubble
F_σ	surface tension force acting on bubble
F_L	liquid inertia force acting on bubble
F_e	Excess internal pressure force due to surface tension
g	gravitational acceleration
h	centroid height from orifice plate
L	height of bubble reference frame from orifice plate (see Fig. 1)
M	Mass of bubble
m_a	orifice mass flowrate
P	pressure
R	bubble equivalent radius
u	radial component of liquid velocity
u_{so}	steam velocity from orifice
U_b	bubble velocity
v	circumferential component of liquid velocity
V_b	bubble volume

greek letters

ρ_a	air density
----------	-------------

ρ_l	liquid density
ϕ_l	liquid potential function
Δt	time interval (between bubble images)
θ	angle between top centre of bubble and position on circumference
α	bubble contact angle at orifice

7 REFERENCES

- [1] Tsuge H. Hydrodynamics of bubble formation from submerged orifices, Encyclopaedia of Fluid Mechanics, (Edited by Cheremisinoff), Vol 3, Chapter 9, 1986
- [2] R.T.Fox, A.T. McDonald, Introduction to Fluid Mechanics, Wiley (1985).
- [3] L.M. Milne Thompson, Theoretical Hydrodynamics, Macmillan, (1965).
- [4] A.S.Ramsey, A Treatise on Hydrodynamics, Part II:Hydrodynamics, G Bell & Sons (1973).
- [5] H.Lamb, Hydrodynamics, Dover Publications (1932).
- [6] A.E. Wraith, T. Kakutani, The pressure beneath a growing bubble, Chem. Eng Sci.Vol. 29 (1974),p 1-12
- [7] Arebi B, The formation and detachment of steam bubbles formed at submerged orifices in sub-cooled water, PhD thesis, University of Strathclyde, Glasgow 1996
- [8] Gray, C The evolution of particle image velocimetry, I.Mech.E Symposium on Optical Methods and Data processing in Heat and Fluid Flow, City University, London 1992